TECHNICAL REPORT ARBRL-TR-02496

A SURVEY OF PENETRATION MECHANICS FOR LONG RODS

Thomas W. Wright

June 1983

US ARMY ARMAMENT RESEARCH AND DEVELOPMENT COMMAND
BALLISTIC RESEARCH LABORATORY
ABERDEEN PROVING GROUND, MARYLAND

Destroy this report when it is no longer needed.
Do not return it to the originator.

Additional copies of this report may be obtained from the National Technical Information Service, U. S. Department of Commerce, Springfield, Virginia 22161.

The findings in this report are not to be construed as an official Department of the Army position unless so designated by other authorized documents.

The use of trade names or manufacturers' names in this report does not constitute indorsement of any commercial product.

UNCLASSIFIED

SECURITY CLASSIFICATION OF THIS PAGE (When Data Entered)

REPORT DOCUMENTATION PAGE		READ INSTRUCTIONS BEFORE COMPLETING FORM
1. REPORT NUMBER TECHNICAL REPORT ARBRL-TR-02496	2. GOVT ACCESSION NO. AD-A131 152	3. RECIPIENT'S CATALOG NUMBER
4. TITLE (and Subtitle) A SURVEY OF PENETRATION MECHANICS FOR LONG RODS		5. TYPE OF REPORT & PERIOD COVERED 6. PERFORMING ORG. REPORT NUMBER
7. AUTHOR(s) T. W. Wright		8. CONTRACT OR GRANT NUMBER(s)
9. PERFORMING ORGANIZATION NAME AND ADDRESS US Army Ballistic Research Laboratory ATTN: DRDAR-BLT Aberdeen Proving Ground, MD 21005		10. PROGRAM ELEMENT, PROJECT, TASK AREA & WORK UNIT NUMBERS
11. CONTROLLING OFFICE NAME AND ADDRESS US Army Armament Research & Development Command US Army Ballistic Research Laboratory (DRDAR-BLA-S) Aberdeen Proving Ground, MD 21005		12. REPORT DATE June 1983 13. NUMBER OF PAGES 43
14. MONITORING AGENCY NAME & ADDRESS(if different from Controlling Office)		15. SECURITY CLASS. (of this report) UNCLASSIFIED 15a. DECLASSIFICATION/DOWNGRADING SCHEDULE

16. DISTRIBUTION STATEMENT (of this Report)

Approved for public release; distribution unlimited.

17. DISTRIBUTION STATEMENT (of the abstract entered in Block 20, if different from Report)

18. SUPPLEMENTARY NOTES

19. KEY WORDS (Continue on reverse side if necessary and identify by block number)

Penetration mechanics, long rods, armor, kinetic energy penetrators

20. ABSTRACT (Continue on reverse side if necessary and identify by block number)

Some of the simpler methods in current use for analyzing ballistic impacts by long rod penetrators are reviewed and critiqued. In spite of several obvious shortcomings the eroding rod model has been used as a starting point and guide for an experimental investigation of penetration phenomena. Some of the principal results of that program are reviewed, and several areas for future work are identified. Carefully developed, time resolved data of the types described in this report should serve as a standard of comparison for large-

DD FORM 1 JAN 73 1473 EDITION OF 1 NOV 65 IS OBSOLETE

UNCLASSIFIED

SECURITY CLASSIFICATION OF THIS PAGE (When Data Entered)

scale computations of penetration phenomena. These data are already being used to guide development of improved engineering models for long rod penetration.

TABLE OF CONTENTS

LIST OF ILLUSTRATIONS

I. INTRODUCTION

Long rod penetrators are modern equivalents of the cannonball, intended to pierce a target by depositing large amounts of kinetic energy in a concentrated region. Typical striking velocities lie in the range of approximately 1-3 km/s. Although a modern penetrator is a machined metal part of some complexity, since it must be fitted with various appurtenances to achieve efficient launch and flight, it may be idealized as a right circular cylinder with a ratio of original length to diameter, L_o/D, greater than some arbitrary number, say ten. The penetrator is intended to fly and to strike its target end on. When the target thickness is greater than a few penetrator diameters, the mechanism of penetration is a complex process in which a cavity is made in the target and the end of the penetrator erodes away. Some of the principal features of impact are shown in Figure 1.

Material response properties under impact conditions are also complex. It has been estimated in a recent report of the National Materials Advisory Board[1] that typical maximum pressures and maximum strain rates during penetration may lie in the ranges 5-50 GPa and 10^4-10^6 s^{-1}, respectively. The higher values are associated with the earliest times after impact and with shock waves, but pressures and strain rates, aided by the presence of nearby free surfaces, quickly decay toward the lower values for the bulk of the process. Since strong armor or penetrator materials may have ultimate stresses of 1-2 GPa, it is apparent that maximum pressures are not orders of magnitude higher than material strengths except perhaps locally for very short periods of time. In fact, because of wave reflections, tensile stresses occur as well. In short, although stresses are high, they are not so high that material properties can be safely ignored. Furthermore, phase changes may occur in some materials, notably Fe and U, high pressures are well known to have a strong influence on flow and fracture characteristics, and strain rates are high enough to affect the response of many materials.

On the other hand, it is by no means clear how many details of physical and material processes are really required in order to achieve accurate and useful ballistic predictions.

There are three levels of analysis currently used in an effort to come to grips with the difficulties outlined above. In order of increasing complexity in the representation of physical and material response phenomena these are: (1) empirical data correlation, (2) engineering analysis, and (3) large-scale computer codes. Each approach is useful, each has its own limitations, and to be effective each must be supported by its own brand of high quality experimentation. In this survey some comments will be made on all three approaches, but emphasis will be placed on one particular engineering model and related experimental results.

II. DATA CORRELATION AND DIMENSIONAL ANALYSIS

At the simplest engineering level the ballistician would like to be able to predict the outcome of an encounter between a penetrator and target.

---

[1] *"Materials Response to Ultra-High Loading Rates," National Materials Advisory Board Publ. NMAB-356, Washington: National Academy of Sciences, 1980.*

A - SHOCK WAVE
B - RAREFACTION
C - SHEAR
D - HIGH-PRESSURE REGION
E - PLASTIC DEFORMATION/SLIP
F - INTERFACE EFFECTS
G - LONGITUDINAL WAVE
H - BENDING WAVE

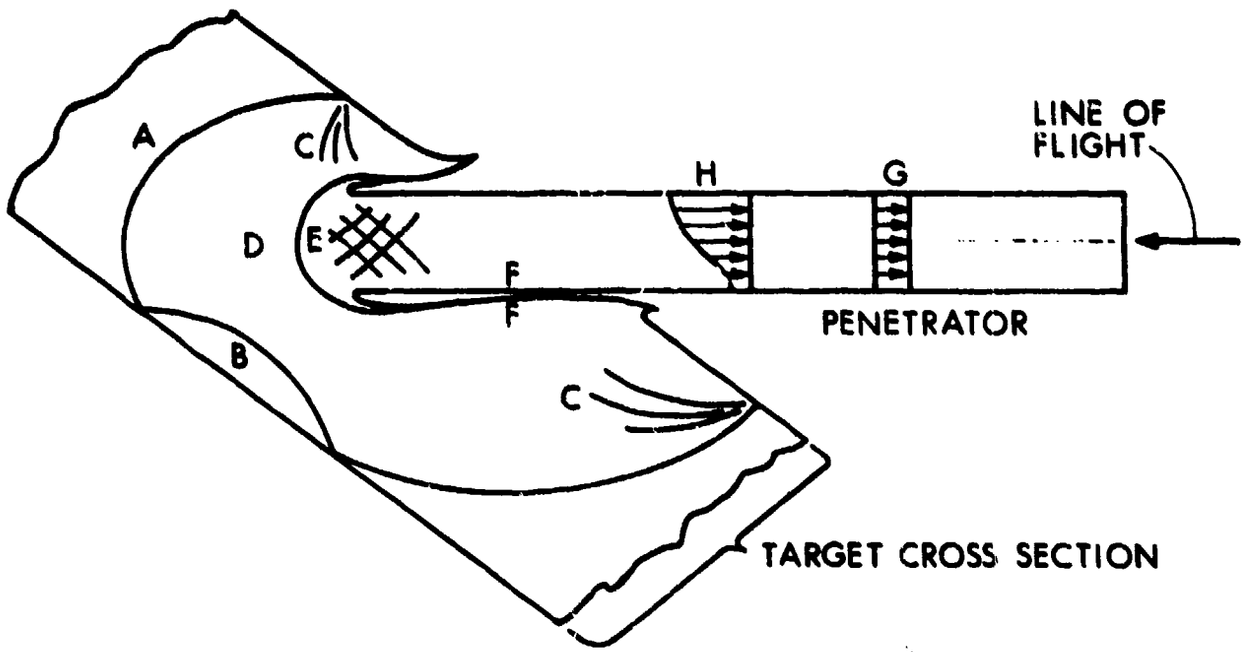

Figure 1. Principal features of long rod penetration.

That is, with given information about geometries and material identifications of both penetrator and target and on line of attack and striking velocity, one would like as a minimum to predict whether or not the target will be perforated, one would like to calculate depth of penetration, and if it is perforated, to calculate residual velocity and residual mass. Consequently, ballistic testing today concentrates on careful control of line of flight and target attitude, and on accurate measurement of striking and residual velocities. When flash X-rays are used for velocity measurements,[2] information is also gained on projectile yaw at impact and line of flight after impact. Often an estimate of residual mass can be made as well.

There have been many attempts to make empirical correlations of ballistic data.[3] Typical cases are listed below in Table I.

TABLE I: Typical Correlation Functions for Ballistic Data

deMarre[4] : $MV_L^2 = CD^\beta T^\alpha$

Grabarek[5]: $MV_L^2/D^3 = C\left(\frac{T \sec\Theta}{D}\right)^\alpha$

Thor[6] : $V_S - V_R = C\, T^\alpha M^\beta V_S^\gamma$

M = projectile mass
D = projectile diameter
T = target thickness
Θ = obliquity, measured from plate normal
α, β, γ, C = empirical, best fit parameters

V_S = Striking velocity
V_R = residual velocity
V_L = limit velocity

---

[2] *F. Grabarek and L. Herr, "X-Ray Multi-Flash System for Measurement of Projectile Performance at the Target," BRL-TN-1634, Ballistic Research Laboratory, APG, MD, 1966 (AD 807619).*

[3] *M. E. Backman and W. Goldsmith, "The Mechanics of Penetration of Projectiles into Targets," Int. J. Eng. Sci., 16, 1-99, 1978.*

[4] *J. deMarre, "Perforation of Iron and Steel Sheets with Normal Firing (Trans.)," Memorial de l'Artillerie de Marine, 14, 1886. Empirical formulas of this type for limit energy are often called deMarre relations, at least in the U.S. In his original paper deMarre gave the formula with $\alpha = 1.4$ and $\beta = 1.5$.*

[5] *C. Grabarek, "Penetration of Armor by Steel and High Density Penetrators," BRL-MR-2134, Ballistic Research Laboratory, APG MD, 1971 (AD 518394L).*

[6] *Project Thor Tech. Report No. 47, "The Resistance of Various Metallic Materials to Perforation by Steel Fragments; Empirical Relationships for Fragment Residual Velocity and Residual Weight," Ballistic Analysis Laboratory, The Johns Hopkins University, 1961.*

These correlations and others like them can be extremely useful for predicting other cases that lie within the same general data set, that is, for data interpolations or even for small extrapolations. It will be noted, however, that none of the three cases cited contains information on material properties. Therefore, every change in material requires a new set of coefficients. In fact, none of the formulae in Table I is even given in nondimensional form, so that the range of applicability in each case is unduly restrictive.

On the other hand, there are many dependent variables of possible interest, and even more independent variables that may influence the outcome of a given encounter. Some of the possibilities are shown in Table II. The rows of dots signify all other possible variables, and each entry in the list of material variables can be given for both penetrator and target. Even with the reduction to nondimensional variables, the analyst is still faced with a bewildering array of possible influences, and because of limitations in both time and money available for testing, it invariably turns out that the test data are incomplete with respect to some variables.

TABLE II: Variables for Dimensional Analysis

Dependent Variables:

P = depth of penetration	M_R = residual mass
V_L = limit velocity	θ_R = angle of residual trajectory
V_R = residual velocity	v_h = hole volume
L_R = residual length	.....

Independent Variables:

Physical Characteristics

L_o = initial length	M_o = initial mass
D = diameter	T = target thickness
.....	

Kinematic Characteristics

V_S = striking velocity	θ_S = angle of striking trajectory
α = angle of yaw	.....

Material Characteristics

Σ_Y = yield stress	ρ = density
Σ_u = ultimate stress	K_{IC} = fracture toughness
h = hardness	
ϵ_u = elongation at Σ_u	.....

Recently an attempt has been made by Bruchey[7] to include more variables than has been customary in the past. The nondimensional form chosen by him for data correlation is given in Eqn. (1).

$$\frac{\rho_p V_L^2}{E_p} \frac{L_o}{D} = C \left(\frac{T \sec\theta}{D}\right)^{\alpha} \left(\frac{E_p}{E_t}\right)^{\beta} \left(\frac{\rho_p}{\rho_t}\right)^{\gamma} . \tag{1}$$

E_p and E_t both have the form

$$E = \frac{1}{2} (\Sigma_Y + \Sigma_u) \epsilon_u , \tag{2}$$

and represent measures of the energy per unit volume that can be absorbed in the penetrator and target materials before rupture occurs. $T\sec\theta$ is the line of sight thickness of the target, and all other quantities are as listed in Table II. The coefficient C and the powers α, β, and γ are determined by a multilinear regression analysis. The total data set includes only 25 separate cases, but within that set there is substantial variation of the nondimensional ratios. The ratio L_o/D varies by a factor of 2, $T\sec\theta/D$ varies by 4, ρ_p/ρ_t varies by 1 1/4, E_p/E_t varies by 5, and ϵ_u varies by 4.

Other groupings of the variables could have been made. For example, instead of the left-hand side of Eqn. (1) as given, the grouping

$$\frac{\rho_p V_L^2 L_o}{E_t T \sec\theta}$$

could have been used. This form may be interpreted as the kinetic energy available per unit area normal to the line of flight compared with the ability of the target to absorb energy per unit area. When this form is used, the powers on the right hand side are all small numbers less than one, indicating only weak dependence, but the overall agreement after the regression analysis is no better than the original result.

For Eqn. (1) the calculated vs. the observed limit velocities are shown in Fig. 2.

For velocity, varying by a factor of 2, agreement is generally within about 10%. For more restricted data sets, that is for data sets with less variation in material and geometric properties, much better agreement can be achieved, but only with a corresponding loss in generality of the correlations.

In that it attempts to incorporate some effect of material properties, Eqn. (1) is an improvement over Table I, but it still uses only a few of the non-dimensional numbers possible from Table II. Furthermore, the assumed

---

[7] *W. Bruchey, Private communication. In preparation as a report, Ballistic Research Laboratory, APG, MD.*

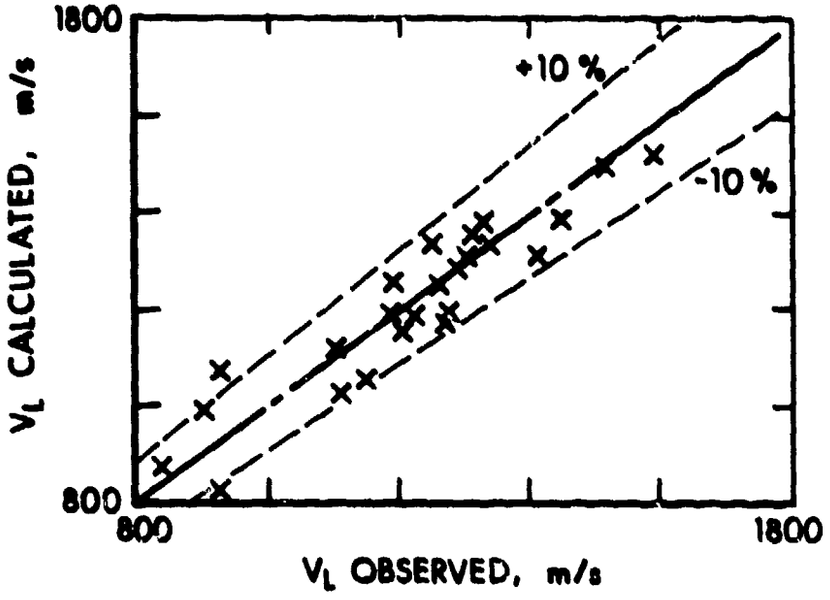

Figure 2. Limit velocity as calculated from Eqn. (1) compared with observed values.

power law relationship among variables is an extremely limited choice of possible functional dependences.

As illustrated in Fig. 3 extrapolation with the weak power law dependence may, and in fact often does, cause substantial error. On the other hand, experimentation to determine general dependence of the form

$$\frac{\rho_p V_L^2 L_o}{E_t T \sec\Theta} = f\left(\frac{T \sec\Theta}{D}, \frac{E_p}{E_t}, \frac{\rho_p}{\rho_t}, \frac{L_o}{D}, \cdots\right), \tag{3}$$

for example, would be an enormous task. A better strategy would be to look for trends within subsets of the available data, where only one variable at a time is allowed to vary, and then to try to fit the data with simple functions that have limited degrees of freedom.

But no matter how the correlations are made, it will be difficult, if not impossible, to gain more than qualitative insight into the nature of the physical processes at work. For a quantitative view of these processes, it is necessary to construct physical models.

III. ENGINEERING ANALYSIS

There have been many attempts to construct simple models of penetration. Many of these are described in a recent survey,[3] but only one, the eroding rod model, will be summarized here, because it has proved useful as a starting point for an experimental program and for further theoretical refinements. The goal for any engineering model is to construct a system of equations with enough detail to be physically realistic but at the same time simple enough for rapid computation.

The eroding rod model in its simplest form was given independently by Alekseevskii[8] and Tate.[9] With the instantaneous length of the penetrator L, speed U, and depth of penetration P, the equations may be written as follows:

Mass: $$\dot{L} = \dot{P} - U \tag{4}$$

Momentum: $$\rho_p L\dot{U} = -\Sigma_p \tag{5}$$

Modified Bernoulli: $$\Sigma_p + \frac{1}{2}\rho_p(U-\dot{P})^2 = \Sigma_t + \frac{1}{2}\rho_t \dot{P}^2 \tag{6}$$

In these equations the only material properties included are flow stress Σ and density ρ where subscripts p and t denote penetrator and target, respectively.

---

[8] *V. P. Alekseevskii, "Penetration of a Rod into a Target at High Velocity," Comb., Expl., and Shock Waves, 2, 63-66, 1966, trans. from Russian.*

[9] *A. Tate, "A Theory for the Deceleration of Long Rods After Impact," J. Mech. Phys. Sol. 15, 387-399, 1967, and "Further Results in the Theory of Long Rod Penetration," J. Mech. Phys. Sol., 17, 141-150, 1969.*

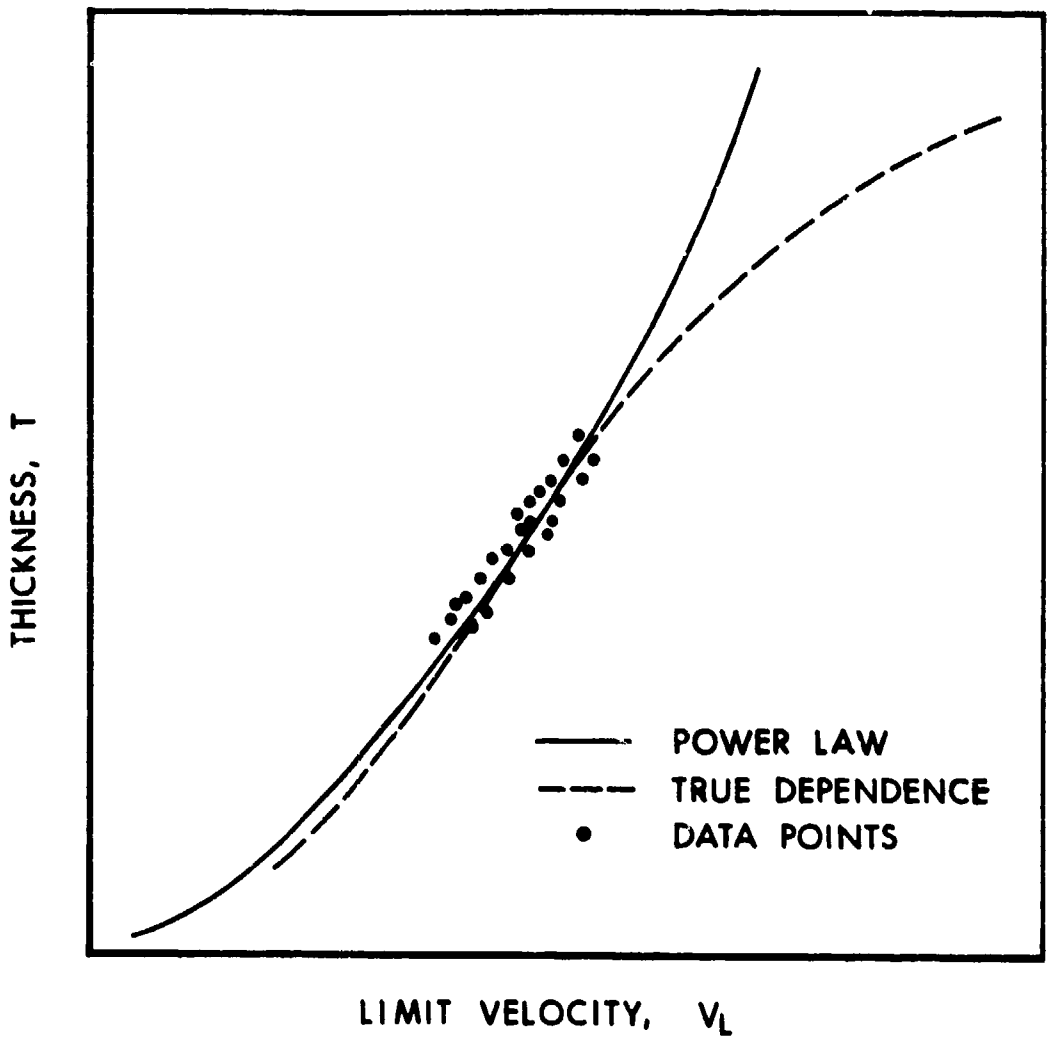

Figure 3. Failure of extrapolation with a power law.

The interpretation of Equations (4) and (5) as balance of mass and balance of linear momentum is straight forward. Equation (6) should be interpreted as showing equality of axial stresses at the interface between penetrator and target on the stagnation line. For the case of steady flow with perfect fluids the expression $p + \frac{1}{2}\rho v^2$ is constant along a steamline. At the stagnation point the velocity relative to that point vanishes so the constant is the interface pressure. If both the rod and target are assumed to behave like perfect fluids in steady flow for some short distance away from the interface where the solid character of each material reasserts itself, then the left side of (6) holds for the rod and the right side for the target with the equality holding because stresses must match at the interface.

Inherent in the model is the assumption that both penetrator and target may be approximated as rigid/plastic materials. That is, either material flows at its characteristic stress Σ or it locks up and doesn't deform at all. For example, if $\Sigma_t > \Sigma_p$, both penetrator and target material flow only if $U > \sqrt{2(\Sigma_t - \Sigma_p)/\rho_p}$. At this critical speed $\dot{P}$ becomes zero and the target ceases to deform, but the penetrator continues to erode until U drops to zero. On the other hand, if $\Sigma_p > \Sigma_t$, both materials flow only if $\dot{P} > \sqrt{2(\Sigma_p - \Sigma_t)/\rho_t}$. When the rate of penetration drops below that speed, erosion of the penetrator stops, $U = \dot{P}$, and the right side of (5) must be replaced by $-(\Sigma_t + \frac{1}{2}\rho_t \dot{P}^2)$. The penetrator then continues to penetrate as a rigid body until U drops to zero.

Equations (4) - (6) are simple enough to be solved on a programmable hand calculator. Typical predictions are shown in Fig. 4 where nondimensional penetration is plotted as a function of nondimensional striking velocity. The qualitative features of the model are striking and useful in themselves. The curve moves to the right for increasing target strength and to the left for increasing penetrator strength, which is in accord with common sense, of course, but the model gives a quantitative estimate of the amount of change as well. All curves have a characteristic S-shape and show a saturation value for high impact speeds. This is in sharp contrast to the shape of the power law curves customarily used for data correlation. The eroding rod model also brings out important natural scaling effects, the most important one being that penetration is proportional to penetrator length if all other properties are held fixed. Thus, to maximize penetration for a penetrator of fixed mass, the ratio L_o/D should be as high as possible, consistent with structural stability and other engineering constraints.

A less obvious consequence of the model is that for a fixed amount of kinetic energy and fixed L_o/D there is an optimum striking velocity that will maximize penetration. That same velocity also minimizes the energy required to achieve a fixed depth of penetration. These facts follow simply from the saturation effect. Penetration may be represented as $P = L_o\, S(U_o)$ where $S(U_o)$ is the S-shaped saturation curve. Then, since kinetic energy K is

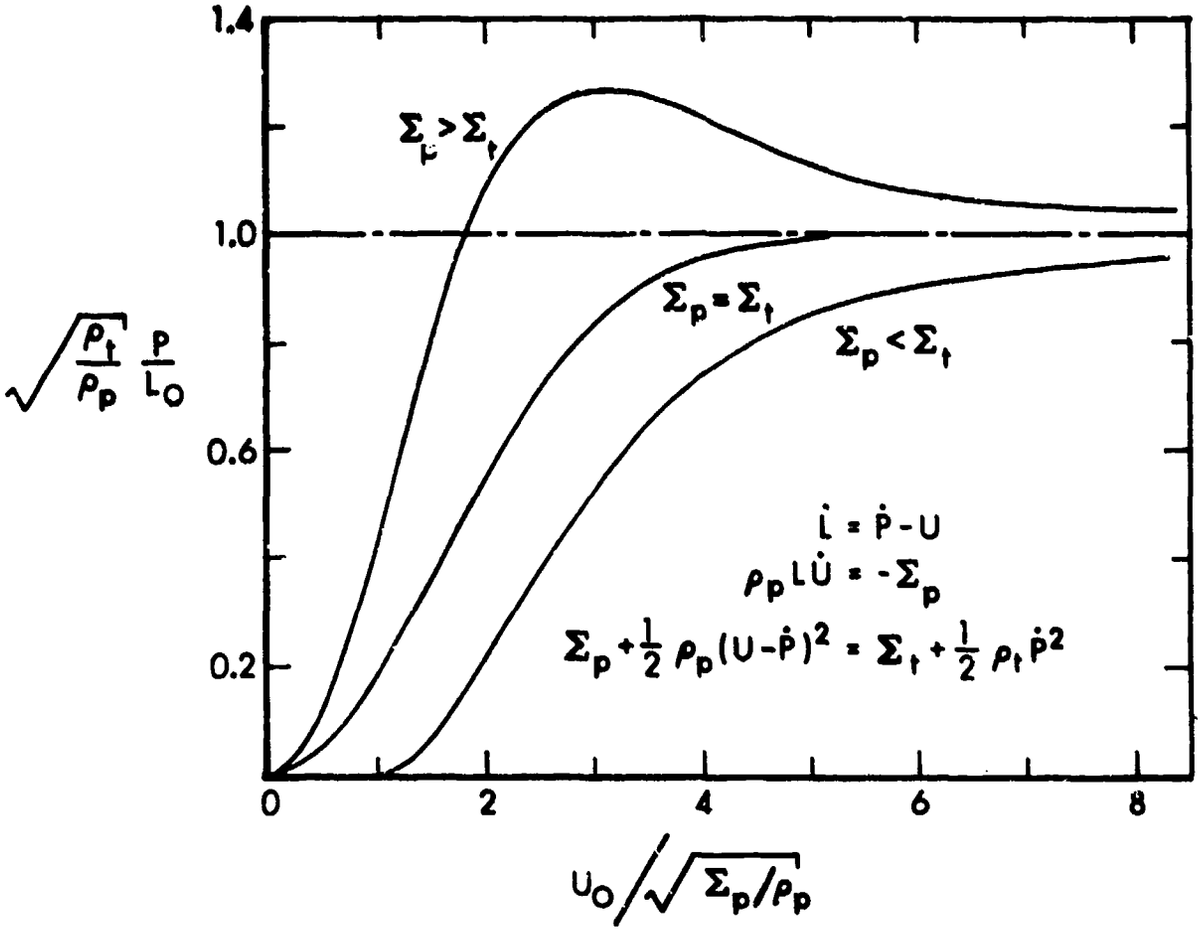

Figure 4. Typical predictions of the eroding rod model.

proportional to $L_o^3 U_o^2$ for fixed L_o/D, the results follow from a minimization problem with side constraint. The optimum velocity is the solution of

$$\frac{dS}{dU_o} = \frac{2}{3}\frac{S}{U_o} , \tag{7}$$

and may easily be found graphically. There will be no solution to (7) if the curve $S(U_o)$ does not bend over far enough so the tendency toward saturation is essential for this result to hold. Results of this kind have previously been given by Frank[10]

Figure 5 shows experimental data reported by Stilp and Hohler[11] Similar data were given by Tate, et al[12] The striking simularity of the experimental curve and the theoretical curve for $\Sigma_p < \Sigma_t$ is clearly evident.

Equations (4) - (6), therefore, have considerable intuitive appeal, combining as they do simplicity with qualitative accuracy, but they are difficult to use quantitatively because values for the characteristic flow stresses are not readily available *a priori*. The usual procedure has been to choose the stresses so as to fit an experimental S-curve, and then to consider them as material constants. Due to approximations inherent in the model, this procedure is unlikely to be satisfactory in all cases. There are several difficulties, nearly all of which are associated with the modified Bernoulli equation itself. These have been described in some detail previously by Wright[13]

The first problem is in the origin of Equation (6). Strictly speaking, the equation only applies for steady flow in perfect fluids. The stresses in the equation would be those that occur at interfaces where the penetrator or target material undergoes a transformation from rigid solid to perfect fluid. Furthermore, the fluid layers must be imagined to have constant thickness so that the fluid/solid interfaces both have the speed $\dot{P}$. Melting can occur in ballistic impact if the speed is high enough, but in any case there will be a region of plastic flow on either side of the penetrator/target interface. For normal impact with the z-axis along the centerline of the rod, the z-component of the momentum equation may be written

---

[10] *K. Frank, "A Qualitative Determination of the Velocity, Mass, and Fineness Ratio Required to Defeat Single Plate Targets," Spring Tech. Conf., Ballistic Research Laboratory, APG, MD, 1978.*

[11] *V. Hohler and A. J. Stilp, "Penetration of Steel and High Density Rods in Semi-Infinite Steel Targets," Third Int. Symp. Ballistics, Karlsruhe, Germany, 1977.*

[12] *A. Tate, K. E. B. Green, P. G. Chamberlain, and R. G. Baker, "Model Scale Experiments on Long Rod Penetrators," Fourth Int. Symp. Ballistics, Monterey, CA, 1978.*

[13] *T. W. Wright, "Penetration with Long Rods: A Theoretical Framework and Comparison with Instrumented Impacts," ARBRL-TR-02323, Ballistic Research Laboratory, APG, MD, 1981 (AD A101344).*

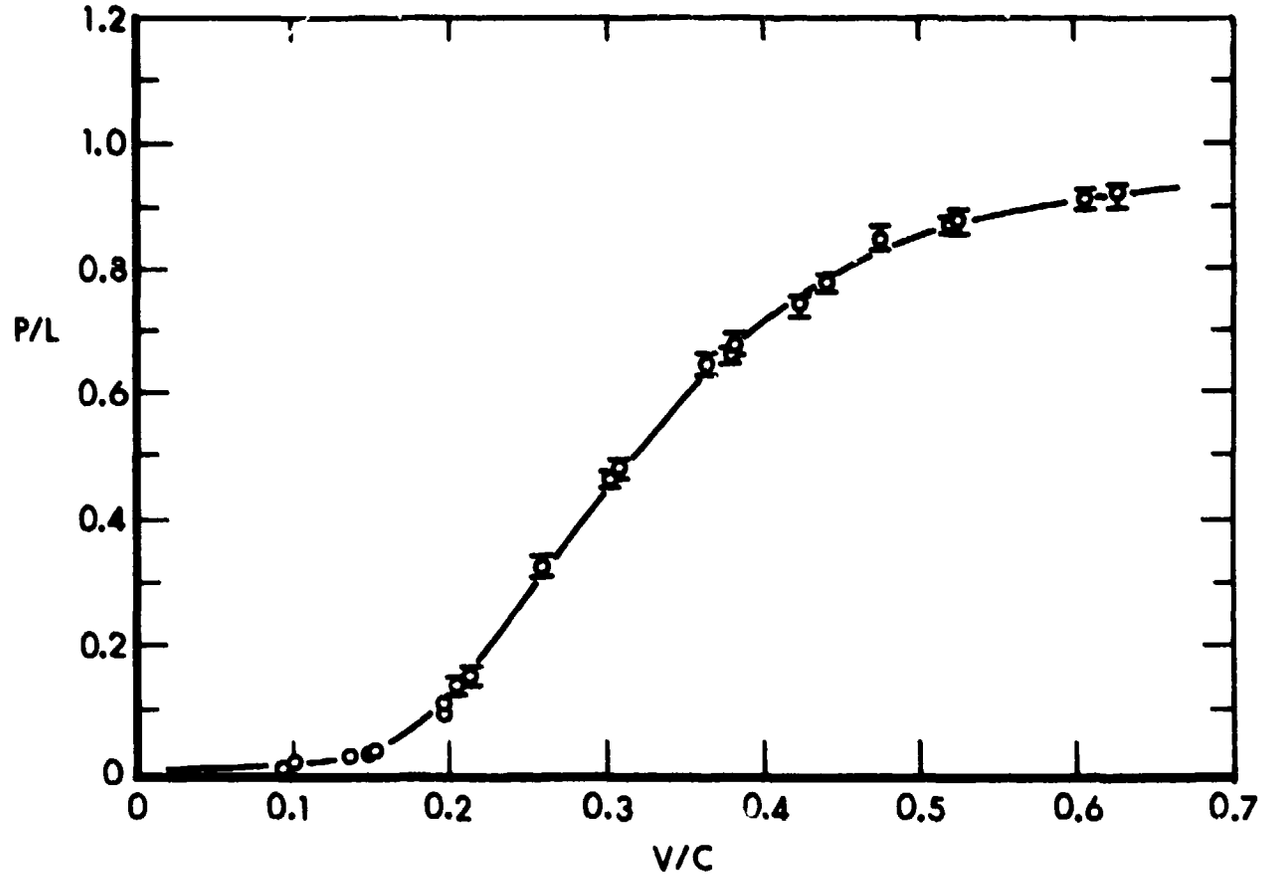

Figure 5. Experimental curve of penetration vs. striking velocity (after Stilp and Hohler[11]).

$$t_{zz,z} + t_{zy,y} + t_{zx,x} = \rho(u_{z,t} + u_x u_{z,x} + u_y u_{z,y} + u_z u_{z,z}) \qquad (8)$$

where the commas denote partial differentiation. On the centerline the transverse components of velocity, u_x and u_y, are zero by symmetry and for steady flow $u_{z,t}$ is zero, also. Shear stresses also vanish on the centerline, but not their derivatives, so integration of Equation (8) between points a and b, assuming incompressibility, yields

$$t_{zz}(b) - t_{zz}(a) + \int_a^b (t_{zy,y} + t_{zx,x})\, dz = \frac{1}{2}\rho\left[u_z^2(b) - u_z^2(a)\right] . \qquad (9)$$

If point b is the stagnation point at the penetrator/target interface, and if point a lies at the rigid/plastic boundary in either penetrator or target, then with $t_{zz}(a) = -\Sigma$ for compressive stresses Equation (6) must be replaced by

$$\Sigma_p + I_p + \frac{1}{2}\rho_p(U-\dot{P})^2 = \Sigma_t + I_t + \frac{1}{2}\rho_t\dot{P}^2 \qquad (10)$$

where I is the integral in Equation (9). If Σ and I are lumped together, then Equation (10) has the same form as Equation (6), but the integrals are undetermined.

A second problem concerns the validity of the assumptions of steady flow and rigid/plastic materials. Taken overall, kinetic energy penetration is clearly an unsteady process, especially in the initiation and final stopping or breakout phases, but there may be parts of the process, localized in both space and time that are nearly steady. For example, during the intermediate stages of penetration a local interaction region may form near the penetrator/target interface, within which Equation (10) holds approximately. If the target is thick enough and the penetrator long enough, this intermediate stage will be the dominant phase of penetration.

Even in such a case, however, there is no clear way to make an accurate estimate of the characteristic stresses from knowledge of measured mechanical properties. The stress/strain curve of most real high-strength materials cannot be well approximated by the rigid/plastic assumption because of work hardening. Furthermore, failure processes in a high rate interaction zone must be regarded as largely unknown so that it is impossible to specify either a maximum strain or a maximum stress at failure with any degree of confidence. Thus, there is at present no well defined way to choose the characteristic flow stresses. Even a criterion based on energy equivalence does not seem particularly feasible.

In addition to the uncertainty concerning flow stresses and the integrals in Equation (10), there is further uncertainty concerning the spherical component of stress in both penetrator and target. The axial stress in Equation (9) or (10) may be decomposed into the sum of a spherical and a deviatoric part. The flow stress is associated only with the latter, but the spherical or hydrostatic part is totally undetermined. In the penetrator nearby free lateral surfaces will tend to minimize the spherical stress, but in the target there are no lateral surfaces, and the hydrostatic component will be the major part of the axial stress.

Still another consequence of real nonrigid material behavior is that there will be considerable plastic deformation at some distance from the quasi-steady interaction zone. In the rod this has the effect of slowing material down before it reaches that zone so that the speed U to be used in Equation (10) is less than that of the rear end. In the target, plastic deformation (including bulging of the rear surface) has the effect of increasing the spatial rate of penetration. Target deformation and bulging has been explicitly included in the model for perforation by rigid projectiles given by Ravid and Bodner.[14]

Finally, inertia will tend to increase the crater size even after the active driving forces have ceased. The effect of crater inertia is particularly pronounced for low ratios of L_0/D or ultra high velocities and has the effect of increasing penetration above the curves calculated in Fig. 4. This effect has been considered by Frank[15] and more recently by Tate[16]

The third and final problem is that the stress tending to decelerate the rod in Equation (5) is an average stress over the cross section, whereas the stress that enters into the modified Bernoulli equation is the local stress on the centerline. These may be somewhat different from each other especially if the integral in Equation (9) is lumped together with the axial stress to give an effective value for Σ.

For all of the above reasons - the origin and meaning of the modified Bernoulli equation, the questionable validity of steady flow and rigid/plastic assumptions, and the inequality of average and centerline stresses - the eroding rod model is difficult to use quantitatively and gives only limited insight into the details of the actual penetrator/target interaction. Nevertheless, in spite of its shortcomings the model appears to contain the germ of a sound theory of penetration for long rods, as shown by the qualitative success of its predictions.

IV. AN EXPERIMENTAL PROGRAM

Penetration is controlled by flow and failure processes that occur at or near the penetrator/target interface. These processes depend only on the material properties of the particular materials involved, and therefore, in large measure they will depend only on the local stress and strain fields, and possibly the gradients or time rates of change of those fields. These ideas are at least compatible with the formation of a region of quasi-steady flow at the interface. Since it is a local phenomenon, it seems reasonable to suppose that the steady conditions established will depend only on the local geometry and the mass flux through the region.

---

[14] *M. Ravid and S. R. Bodner, "Dynamic Perforation of Viscoplastic Plates by Rigid Projectiles," Report of the Material Mechanics Laboratory, Technion, Haifa, Israel, 1982.*

[15] *K. Frank, Unpublished Work. His essential idea was to combine the results of the eroding rod model with hypervelocity cratering results of Christman and Gehring, J. Appl. Phys., 37, 1579-1587, 1966.*

[16] *A. Tate, "Extensions to the Modified Hydrodynamic Theory of Penetration," Preprint, to be published.*

With the ideas of the preceding paragraph as a working hypothesis several experiments have been devised to begin probing the details of the interaction process. Obviously, measurements cannot be made directly in the interaction region, but they can be made in both penetrator and target in material immediately adjacent to it. In fact, in terms of the modified Bernoulli equation, it has been possible to make independent measurement of Σ_p, Σ_t, U, and $\dot{P}$.

A. Experiments with Instrumented Rods.

In the first of these experiments, done by Hauver[17,18] and Hauver and Melani,[19] strain gages are placed on the long rod penetrators and strain-time histories are recorded at several stations on the rod. Then from the one-dimensional theory of wave propagation it is possible to reconstruct the stress and particle velocity histories throughout the rod. This is done as follows. The simplest equations for 1-D wave propagation may be written

$$\Sigma_{,Z} = \rho \dot{W}_{,t} \; ; \qquad \dot{W}_{,Z} = \varepsilon_{,t} \tag{11}$$

where Σ is the average axial stress in the rod (referred to the initial cross section), ρ is the initial density, $\dot{W}$ is the particle velocity, and ε is engineering strain. The spatial location, z, is a function of the material particle, Z, and time, t, so that

$$z = z(Z,t), \qquad \dot{W} = z_{,t} \qquad \varepsilon = z_{,Z} - 1 \tag{12}$$

With ε-t data for several stations at hand curves of constant strain may be plotted in Z-t space. Along such a curve the slope, c_p, called the plastic wave speed, may be measured.

$$d\varepsilon = \varepsilon_{,t}\, dt + \varepsilon_{,Z} dZ = 0 \tag{13}$$

$$\frac{dZ}{dt} = c_p = -\frac{\varepsilon_{,t}}{\varepsilon_{,Z}} \tag{14}$$

These curves need not be straight lines, but if they are, as all experiments to date indicate, the analysis is greatly simplified because c_p then depends only on ε. Typical data is shown in Fig. 6, taken from Hauver.[18] The actual experiments were performed in a 4" light gas gun with the penetrator stationary for ease of instrumentation and the target plate launched from the 4" gun. The experiment is shown schematically in the figure.

---

[17] *G. E. Hauver, "Penetration with Instrumented Rods," Int. J. Eng. Sci., 16, 871-877, 1978.*

[18] *G. E. Hauver, "Experiments with Instrumented Long-Rod Penetrators," Fifth Int. Symp. Ballistics, Toulouse, France, 1980.*

[19] *G. E. Hauver and A. Melani, "Strain-Gage Techniques for Studies of Projectiles During Penetration," ARBRL-MR-03082, Ballistic Research Laboratory, APG, MD, 1981 (AD A098660).*

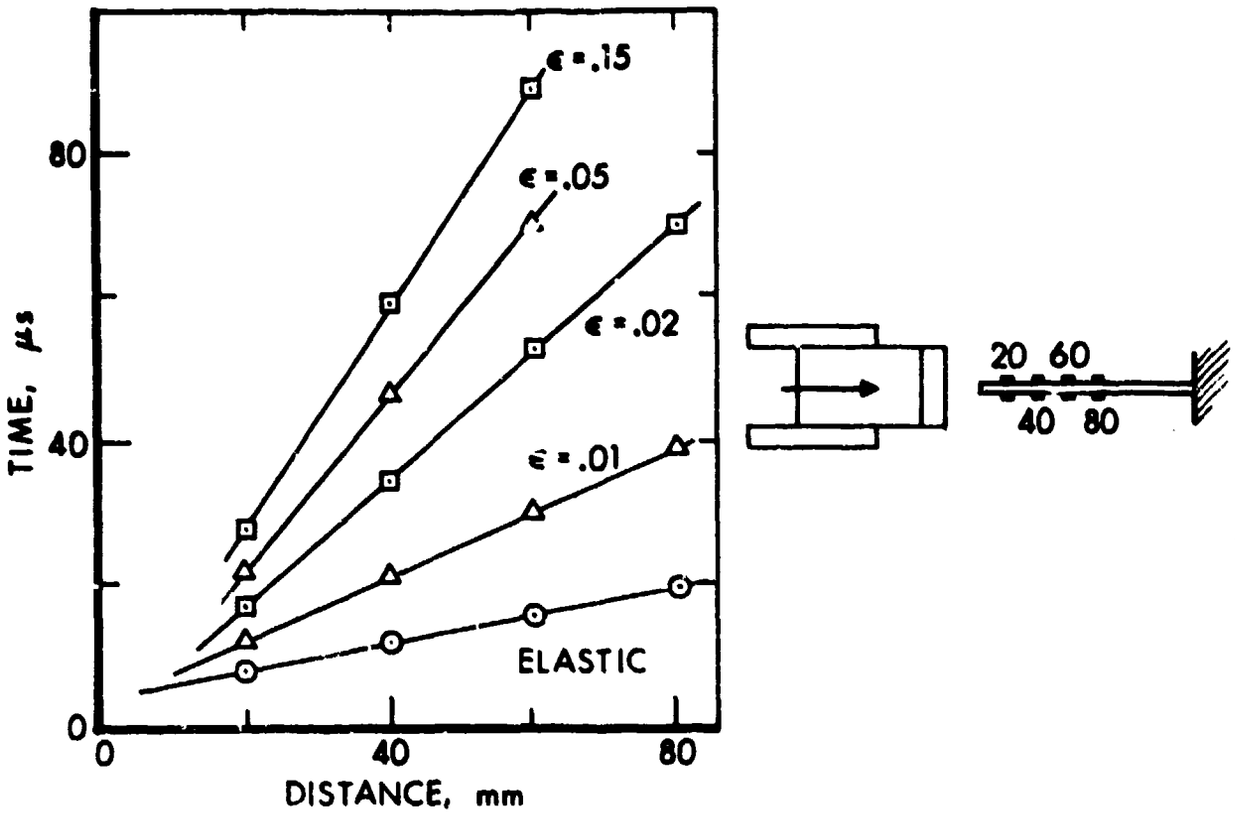

Figure 6. Curves of constant strain in rod coordinates for a high-strength steel rod and an armor steel target. Impact speed was 1000 m/s.

Equations (11) may be integrated with respect to Z along lines t = constant as has been described by Kolsky[20] and others. If the rod has speed $\dot{W}_o$ and zero stress and strain at any station before a wave arrives, we have

$$\dot{W}(Z,t) = \dot{W}_o - \int_o^{\varepsilon(Z,t)} c_p(\varepsilon)\, d\varepsilon, \tag{15}$$

$$\Sigma(Z,t) = \int_o^{\varepsilon(Z,t)} \rho c_p^2\, (\varepsilon)\, d\varepsilon. \tag{16}$$

Note that the stress can be obtained from Equation (16) without recourse to any constitutive assumption. Typical results obtained by Hauver[17,18] and Hauver and Melani[19] are shown in Fig. 7.

The most striking and immediately obvious feature of these results is that the stress, as computed from experiment, does not agree with the measured static stress and in fact the computed stress depends on the striking velocity, V. On the other hand, the particle velocity, as computed from the experiment, agrees well with other experiments also conducted by Hauver and Melani[19] in which particle motion was determined directly by observing fiducial lines on the penetrator with a streak camera. It is not possible to measure stresses directly, but within the limitations of Equations (11), there is no reason to believe that computed stresses are less accurate than computed particle velocities.

Two reasons have traditionally been given for discrepancies between static and dynamic determinations of stress/strain relations. The first, viscoplastic or rate effects, has been ruled out as a major contributor for the penetrator material in this case. Standard Hopkinson bar tests, as reported by Chou,[21] have not shown significant rate effects. The second possibility, the effect of finite radius, must therefore be explored.

Motivated by the results described above, Wright[22] has examined a higher order rod theory where radial strain, u, is treated as an internal variable, and given equal status with the axial displacement, W, as a dependent variable. Either by use of a variational principle to arrive at a one-dimensional formulation directly, or by integration of the three-dimensional equations through a cross section, one can arrive at a coupled pair of one-dimensional equations.

---

[20] *H. Kolsky, "Stress Waves in Solids," New York, Dover Publ., 1963.*

[21] *P.-C. Chou, Letter Report to Ballistic Research Laboratory from Army Mechanics and Materials Research Center, 1980.*

[22] *T. W. Wright, "Nonlinear Waves in Rods," Proc. IUTAM Symp. on Finite Elasticity, D. E. Carlson and R. T. Shield (eds.), The Hague, Boston, London, Nijhoff Publishers, 1980.*

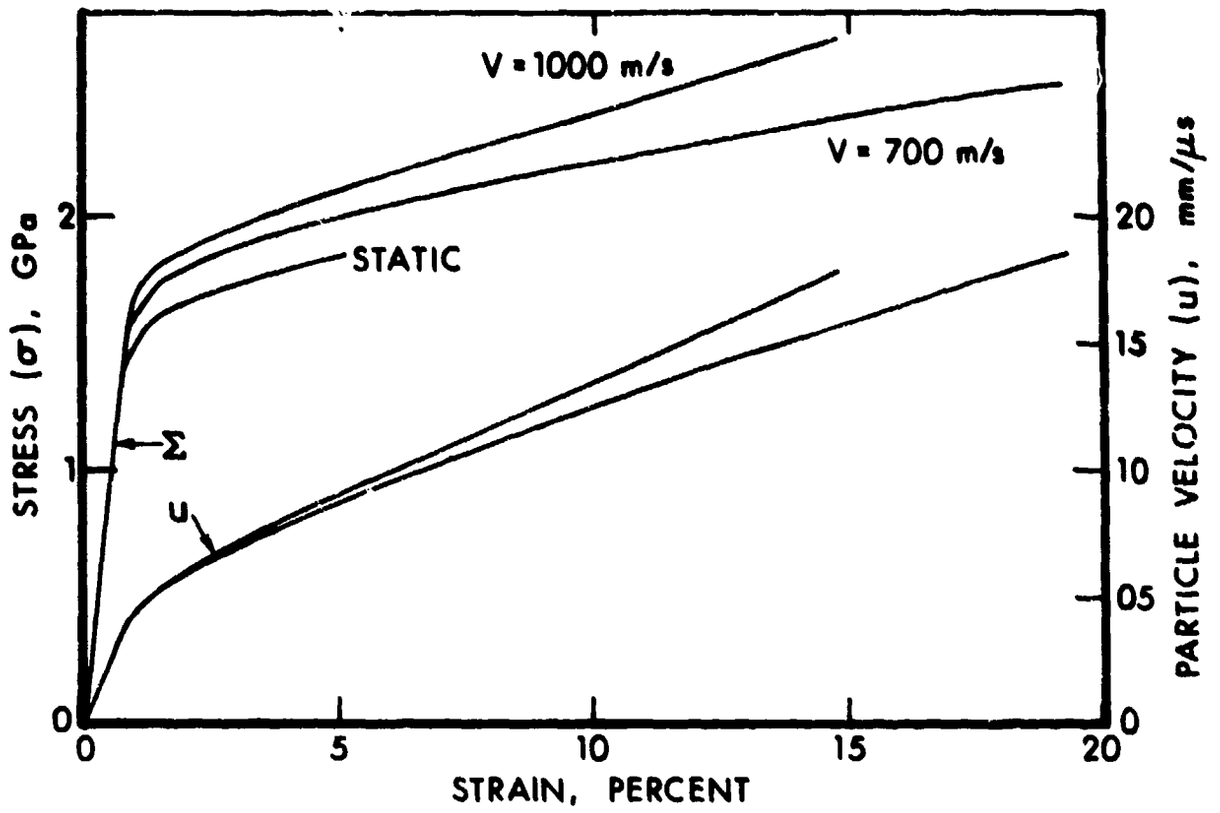

Figure 7. Calculated stress and particle velocity for rod in Fig. 6 at two impact speeds. Also shown is the measured quasi-static stress/strain curve for the rod.

$$\frac{\partial S}{\partial Z} = \rho \frac{\partial^2 W}{\partial t^2} , \tag{17}$$

$$\frac{\partial Q}{\partial Z} - P = \frac{1}{2} \rho a^2 \frac{\partial^2 u}{\partial t^2} . \tag{18}$$

Here S is the average axial stress, P is the average lateral pressure on the rod, Q is the average polar moment of radial shear stress, a is the initial radius of the rod, and ρ, u, and W are as previously defined. In the constitutive equations for S, P, and Q the basic kinematic variables are the axial strain, $\frac{\partial W}{\partial Z}$, the radial strain, u, and the gradient of radial strain, $\frac{\partial u}{\partial Z}$. Analysis of these equations yields quantitative and qualitative information about the structure of wave-like solutions, either for the nonlinear elastic case as in Reference 22 or for the elastic/plastic case, which is currently being studied.

Note that Equation (17) is the same as Equation $(11)_1$. Furthermore, Equation $(11)_2$ applies as a compatibility condition in the present context as well as previously. Therefore, in the treatment of experimental data Equations (15) and (16) are still valid for the computation of particle velocity and stress in the wave. Now, however, there should be no surprise that the stress, as computed for the dynamic case, does not agree with the static curve since the radial strain is still completely undetermined. Analytically it can only be determined through the coupling with Equation (16), which describes the radial motion of the rod.

Since stress is also constant along the lines of constant strain in Fig. 6, it would be possible to determine the load history on the end of the eroding penetrator provided that extent of erosion is known as a function of time and that the erosion trajectory cuts across the straight lines. No experiment has yet been devised to measure extent of erosion directly, but an indirect approach seems possible by determining target penetration as a function of time and matching that curve with the projected arrival trajectories of various rod stations.

B. Experiments to Measure Penetration.

Using the same penetrator and target materials and the same impact conditions as were used by Hauver, Netherwood[23] attempted in a second series of experiments to measure rate of penetration by means of insulated switch wires which were inserted in small holes drilled into the side of the target block. The situation is sketched in Fig. 8. The penetrator is launched by a 4" gas gun, and the switch wires short out in order upon arrival of the penetrator at their target stations. Typical data are shown in Fig. 8 with the upper and lower curves representing bounds on the data over several repetitions of the test with switch pins located at different stations for different tests. Distance is measured with respect to the undeformed target and, therefore, is

---

[23] *P. H. Netherwood, "Rate of Penetration Measurements," ARBRL-MR-02978, Ballistic Research Laboratory, APG, MD, 1979 (AD A080541).*

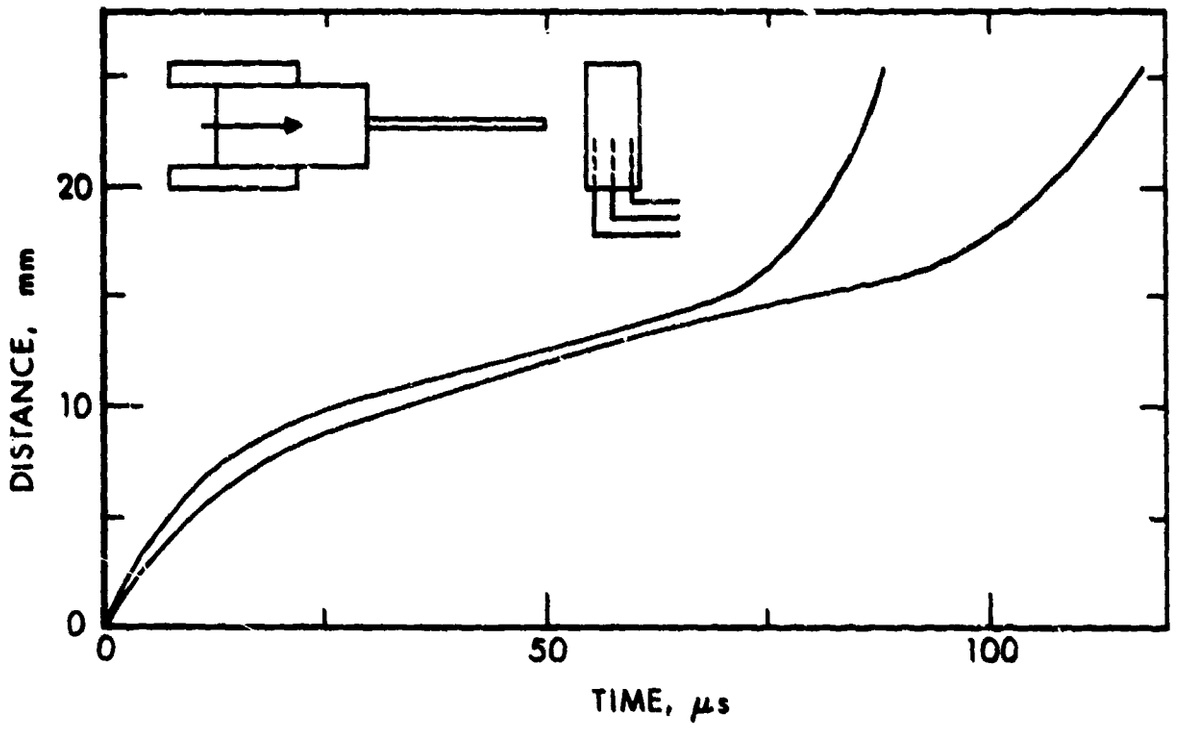

Figure 8. Measured penetration vs. time for same rod and target as in Fig. 6.

a material coordinate. The curves show a rapid entry zone, followed by a nearly steady zone of slow penetration. The last part of the curves should not be interpreted as a rapid exit zone, but rather as an erratic failure zone where a small plug forms near the rear target surface and shears off the switch pins before actual arrival of the penetrator. The erratic behavior is believed to be caused by the somewhat random nature of material failure.

The detailed shape of the curves in Fig. 8 cannot be taken too literally because plastic flow of target material may well cause the switch pins to trigger before penetrator arrival. Clearly, however, the real curve must lie on or below the apparent curve so that the data give an upper bound for depth of penetration at any time. The straight, middle portion of the apparent curve might be supposed to lie parallel to the real curve where quasi-steady flow occurs, but doubt has been cast on that interpretation, as well, by Hauver's recent work.[18] It seems fair to say that truly definitive measurements of penetration vs. time have yet to be made, although Netherwood's experiments represent a major step in that direction.

To compare the penetration curve with the projected arrival trajectories of various rod stations it is necessary to use a common coordinate system. The rod data were taken in the material coordinates of the rod, and the target data were taken in the material coordinates of the target, but both sets of data, as well as the curves of constant strain, may be transformed into a common spatial or laboratory coordinate system.

In material coordinates for the penetrator, the trajectories of constant strain may be written as $Z = Z(t)$ so from use of Equation (12), the trajectories in spatial coordinates may be represented as $z = z(Z(t), t)$. These have slope

$$\frac{dz}{dt} = \frac{\partial z}{\partial t} + \frac{\partial z}{\partial Z}\frac{dZ}{dt} \tag{19}$$

The first term on the right-hand side is given by Equation (15), and the second term is the product of $(1 + \varepsilon)$ and c_p by Equations $(12)_3$ and (14). Therefore, in spatial coordinates the trajectories of constant strain have speed $\frac{dZ}{dt}$ as follows.

$$\frac{dZ}{dt} = \dot{W}_o - \int_o^{\varepsilon} c_p \, d\varepsilon + (1 + \varepsilon)\, c_p. \tag{20}$$

Equation (20) shows that if c_p depends only on ε, these trajectories are straight lines in spatial coordinates as well as material coordinates. Several lines of constant strain are shown in Fig. 9. Note that as penetration occurs, the higher strain levels are actually carried into the target cavity.

The spatial trajectory of any rod station may be computed by integrating Equation (15) with respect to time, Z being held fixed. All that is needed is the strain history at a fixed rod station, and those histories are available either directly from the strain gage records or by interpolation from Fig. 6. Some trajectories of this kind are also shown in Fig. 9. Note that the retardation due to axial compression is clearly visible. The trajectory labeled 96 mm corresponds to the initial length of the recovered penetrator as determined by weighing in one particular test.

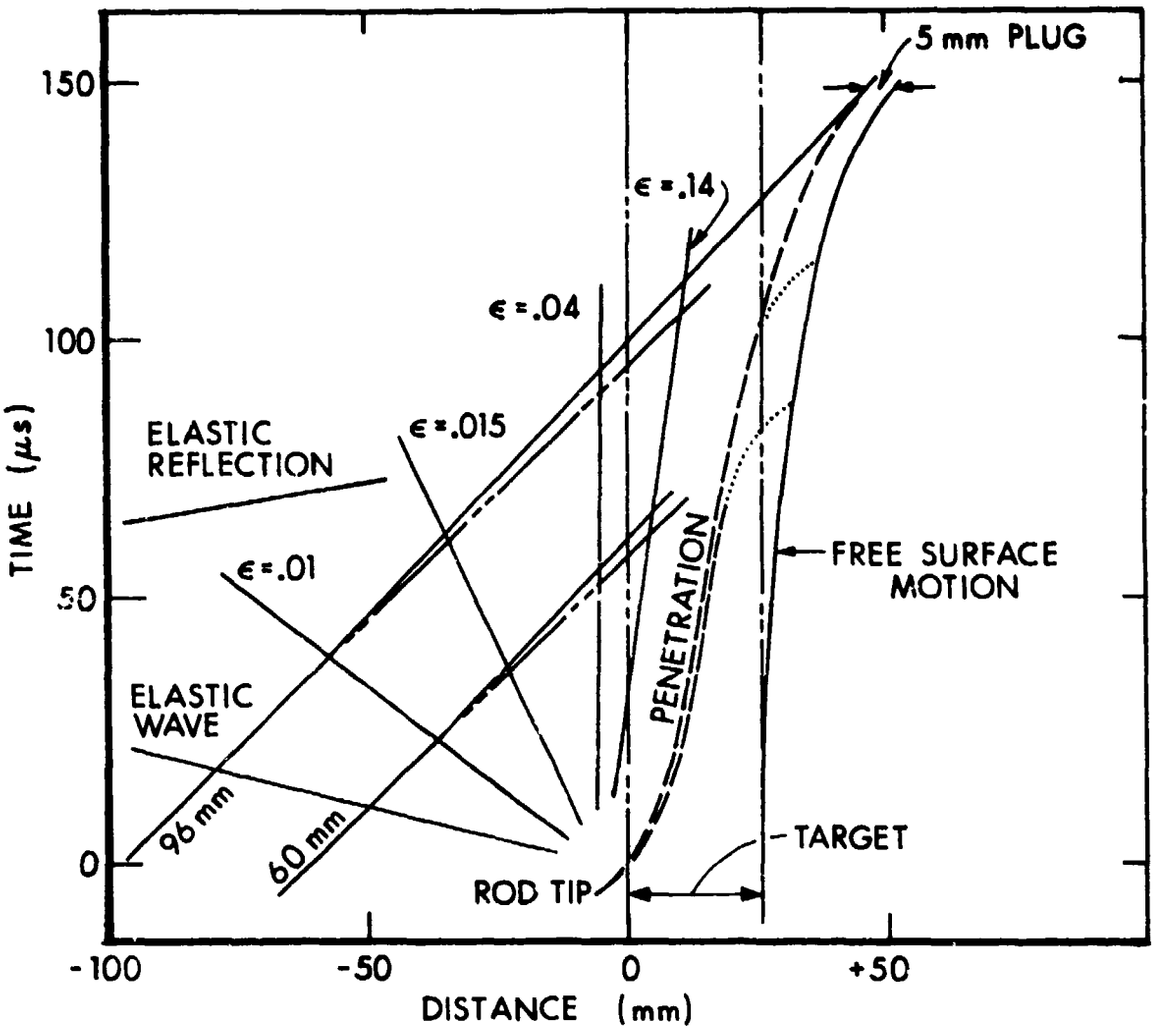

Figure 9. Composite penetration diagram in laboratory coordinates.

Finally, the spatial trajectory of penetration is also shown in Fig. 9. This has been drawn simply by translating the points of the material trajectory by the amount of the free surface motion at corresponding times, ignoring any compression of target material between the penetrator and the free surface. Surface motion was measured by Netherwood, using a streak camera, and in some of his tests a small plug approximately 5 mm in thickness was also recovered.[24]

The trajectories of the 96 mm station, the free surface, and penetration, together with the known plug thickness, form a remarkably coherent picture, and show with graphic clarity the need to account for deformation in a sound physical theory of penetration. That need is evident in spite of the uncertainty in locating the penetration curve.

The highest strains measured all propagate with nearly the same speed. In Fig. 9 that speed appears to be slightly less than the rate of penetration so that it is not clear from the experiments where the erosion trajectory should be shown in Fig. 8. A good approximation is probably a straight line drawn slightly to the left of the highest strain shown, but with a slightly greater slope.

C. Experiments to Measure Target Stress.

In a third series of experiments Pritchard[25,26,27] has measured the stress in the target normal to the path of penetration and directly on the path. A sketch of the experiment is shown in Fig. 10. A manganin foil stress gage was placed in the center of a split rod, the rod was inserted into a hole drilled in the target, and the alignment was adjusted so that the gage lay directly on the line of penetration. This experiment was also performed in a 4" light gas gun. Since the manganin gage is subjected to a diverging strain field, it is necessary to compensate by measuring strain independently and correcting the pressure determination. This is done with a constantin gage, which is actually interleaved with the manganin gage. Details have been given by Pritchard.[25,26]

Typical data are shown in Fig. 10 for a tungsten alloy rod and a steel target.[27] Stress histories begin with shock arrival and increase until gage failure some time before actual arrival of the penetrator. Notice that there is no sharp jump in stress at shock arrival, at least for these cases in which the penetrator had a hemispherical nose, and that the rate of increase is more rapid for the shallower gage location. For the two records shown, gages failed

---

[24] *P. H. Netherwood, Private Communication, 1979.*

[25] *D. S. Pritchard, "Measurements of Dynamic Stress and Strain Components in Targets Struck by Penetrators," ARBRL-MR-03095, Ballistic Research Laboratory, APG, MD, 1981 (AD A100724).*

[26] *D. S. Pritchard, "Piezoresistive Gauge Measurements in Deforming Environments During Penetration," Proc. First Symp. on Gauges and Piezoresistive Materials, Arcachon, France, 1981.*

[27] *D. S. Pritchard and G. E. Hauver, Private Communication of Unpublished Data, 1982. The raw data were taken by Pritchard and reduced and analyzed by Hauver.*

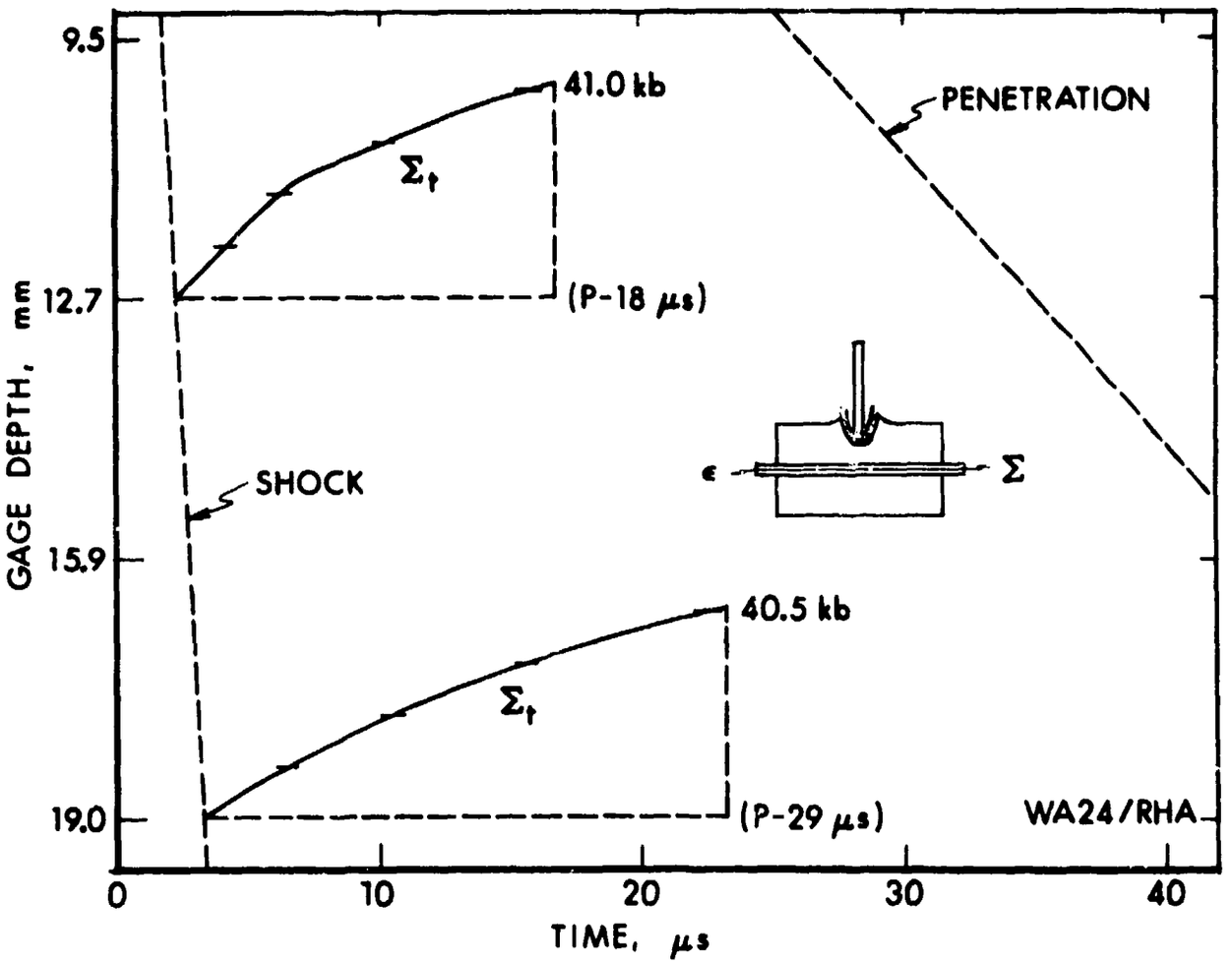

Figure 10. Measured target stress vs. time at depths of 12.7 mm and 19.0 mm below the impact surface. The rod is a tungsten alloy and the target is armor steel.

at less than half the time to penetrator arrival so that extrapolation to penetrator arrival is hazardous at best. Nevertheless, it is at least interesting to note that reasonable extrapolations give a peak stress that is roughly in the range of 50-55 kb for both curves. Data have also been reported for the same combination of materials shown in Fig. 6. The general trend of the data is the same as Fig. 10, but the quality of the data is not as high. (See References 25 and 26.)

V. OTHER CONSIDERATIONS

The experiments described above go a long way towards indicating the phenomena that should be included in a reasonable theory of long rod penetration, but there are other important considerations as well. These may be grouped into three sets of phenomena: hole growth in the target, the failure and discard of eroded penetrator material, and the effects of bending.

Neither the eroding rod model nor any of the experiments described above gives any consideration to the dynamics of hole growth, although some attention has been devoted to this problem in the literature, e.g., Hanagud and Ross[28] or Ravid and Bodner.[14] As the penetrator moves through the target, target material must flow to the sides around the penetrator. At the lower rates of penetration, the extent of lateral motion must be at least great enough to admit passage of the eroded and discarded penetrator material, if any. At higher rates, inertia may drive both target and eroded penetrator material somewhat away from the sides of the remaining intact penetrator, or in the case of a noneroding penetrator, inertia may cause separation of the flow between target and penetrator.

Ductility and fracture characteristics also have a significant effect on penetration. For example, a very ductile material may simply pile up on the target surface at low impact velocities or actually turn inside out to form a tube as it penetrates at higher velocities. (See Reference 29.) In any case, excessive penetrator ductility tends to increase the contact area between penetrator and target, thus providing a larger retarding force to the penetrator. In attempting to simulate numerically some of Hauver's data on instrumented rods, Misey[30] found that it was essential to include at least a crude fracture criterion in his two-dimensional code. Without a fracture criterion the computed strains in the penetrator increased much more rapidly than the experimental data indicated. This would seem to indicate that a fracture criterion would also be useful in an engineering model of penetration.

---

[28] *S. Hanagud and B. Ross, "Large Deformation, Deep Penetration Theory for a Compressible Strain-Hardening Target Material," AIAA Journal, 9, 905-911, 1971.*

[29] *K. Frank, Private Communication on test results.*

[30] *J. J. Misey, A. D. Gupta, and J. D. Wortman, "Comparison of Penetration Codes for Strain Measurements in Kinetic Energy Penetrators," ARBRL-TR-02231, Ballistic Research Laboratory, APG, MD, 1980 (AD A084391).*

Finally, in any complete engineering theory of penetration some consideration must be given to the effects of bending as induced by oblique impact or penetrator yaw at impact, and should include lateral stability or bending enhancement due to axial loading. A start was made by Abrahamson and Goodier,[31] who considered lateral stability of an elastic/linear work hardening rod in normal impact on a rigid target. However, they did not consider the effect of moments or transverse forces at the impact end as might be induced by yaw and obliquity, and even more important from the point of view of penetration mechanics, they did not include the effect of penetrator erosion, which in effect provides a moving boundary for the application of forces and moments. No thorough experimental study on bending effects seems to have been undertaken, although limited data exists, Hauver.[17]

VI. COMPUTER CODES

The third approach to penetration mechanics uses large scale numerical simulation with the full equations of continuum physics. The characteristics of some typical codes and their limitations have been described by Zukas[32] and Jonas and Zukas[33] so that only a few comments are required here. The ordnance regime still remains today as extremely difficult for making accurate numerical predictions, especially for impact speeds near the limit velocity. This difficulty is commonly attributed to lack of adequate knowledge concerning both dynamic material properties and fracture descriptions in the codes. (See Reference 33 for example.) The determination of deformation and fracture properties at high pressures and high rates of strain requires exceptional experimental skill and ingenuity, especially since the dynamic situation makes it all but impossible to determine constitutive properties without imposing *a priori* constitutive models or assumptions. There is always some circularity in the common procedure of "backing out" constitutive properties by choosing free parameters in a given model so as to obtain rough agreement between a calculation and experimental data. On the other hand, there often seems to be little other choice. All that can be asked is that critical judgment and restraint be used in interpreting and accepting results. Reference 1 gives a thorough review of current practice in constitutive modeling for codes and recommends avenues for future improvements.

As constitutive models become more comprehensive, ever greater burdens will be placed on computing capacity, which must be offset either by increases in machine size and speed or by increases in the efficiency of computing algorithms. Computing power should be reserved for those parts of the problem

---

[31] *G. R. Abrahamson and J. N. Goodier, "Dynamic Flexural Buckling of Rods within an Axial Compression Wave," J. Appl. Mech., 33, 241-247, 1966.*

[32] *J. A. Zukas, "Numerical Simulation of Impact Phenomena" (Chap 10), "Three-Dimensional Computer Codes for High Velocity Impact Simulation" (Chap 11), in Impact Dynamics, J. A. Zukas, T. Nicholas, H. F. Swift, L. B. Greszczuk, D. R. Curran, New York, Wiley-Interscience, 1982.*

[33] *G. H. Jonas and J. A. Zukas, "Mechanics of Penetration: Analysis and Experiment," Int. J. Eng. Sci., 16, 879-903, 1978.*

that most need it, and not wasted on regimes where little is happening. Fortunately, rapid advances are being made in both hardware and software so that advances in constitutive modeling can be expected to be implemented in penetration calculations.

VII. CONCLUSIONS

The three current approaches to penetration mechanics - data correlation, engineering models, and large scale computer codes - will all continue to evolve with increasing emphasis being placed on the role of material properties and the mechanics of material deformation and failure in each case. In many respects the approach using engineering models is the least developed of the three, but it holds the promise of encompassing virtually all of the relevant physics, yet at far less computational cost than the large-scale codes. The benefit comes from one-dimensional rather than three-dimensional numerical simulation. Data correlations will still be indispensable for organizing large volumes of ballistic data, but engineering models can be expected to suggest improved functional forms for nondimensional analysis. The engineering models themselves should play their biggest role in aiding designers and systems analysts. The large codes will remain as the indispensable tool for examining the details of interaction, and as constitutive models improve, may well permit actual material design for ballistic applications.

REFERENCES

1. "Materials Response to Ultra-High Loading Rates," National Materials Advisory Board Publ. NMAB-356, Washington: National Academy of Sciences, 1980.

2. C. Grabarek and L. Herr, "X-Ray Multi-Flash System for Measurement of Projectile Performance at the Target," BRL-TN-1634, Ballistic Research Laboratory, APG, MD, 1966 (AD 807619).

3. M. E. Backman and W. Goldsmith, "The Mechanics of Penetration of Projectiles into Targets," Int. J. Eng. Sci., 16, 1-99, 1978.

4. J. deMarre, "Perforation of Iron and Steel Sheets with Normal Firing (Trans.)," Memorial de l'Artillerie de Marine, 14, 1886. Empirical formulas of this type for limit energy are often called deMarre relations, at least in the U.S. In his original paper deMarre gave the formula with $\alpha = 1.4$ and $\beta = 1.5$.

5. C. Grabarek, "Penetration of Armor by Steel and High Density Penetrators," BRL-MR-2134, Ballistic Research Laboratory, APG, MD, 1971 (AD 518394L).

6. Project Thor Tech. Report No. 47, "The Resistance of Various Metallic Materials to Perforation by Steel Fragments; Empirical Relationships for Fragment Residual Velocity and Residual Weight," Ballistic Analysis Laboratory, The Johns Hopkins University, 1961.

7. W. Bruchey, Private Communication. In preparation as a report, Ballistic Research Laboratory, APG, MD.

8. V. P. Alekseevskii, "Penetration of a Rod into a Target at High Velocity," Comb., Expl., and Shock Waves, 2, 63-66, 1966, trans. from Russian.

9. A. Tate, "A Theory for the Deceleration of Long Rods After Impact," J. Mech. Phys. Sol., 15, 387-399, 1967, and "Further Results in the Theory of Long Rod Penetration," J. Mech. Phys. Sol., 17, 141-150, 1969.

10. K. Frank, "A Qualitative Determination of the Velocity, Mass, and Fineness Ratio Required to Defeat Single Plate Targets," Spring Tech. Conf., Ballistic Research Laboratory, APG, MD, 1978.

11. V. Hohler and A. J. Stilp, "Penetration of Steel and High Density Rods in Semi-Infinite Steel Targets," Third Int. Symp. Ballistics, Karlsruhe, Germany, 1977.

12. A. Tate, K. E. B. Green, P. G. Chamberlain, and R. G. Baker, "Model Scale Experiments on Long Rod Penetrators," Fourth Int. Symp. Ballistics, Monterey, CA, 1978.

13. T. W. Wright, "Penetration with Long Rods: A Theoretical Framework and Comparison with Instrumented Impacts," ARBRL-TR-02323, Ballistic Research Laboratory, APG, MD, 1981 (AD A101344).

14. M. Ravid and S. R. Bodner, "Dynamic Perforation of Viscoplastic Plates by Rigid Projectiles," Report of the Material Mechanics Laboratory, Technion, Haifa, Israel, 1982.

15. K. Frank, Unpublished Work. His essential idea was to combine the results of the eroding rod model with hypervelocity cratering results of Christman and Gehring, J. Appl. Phys., 37, 1579-1587, 1966.

16. A. Tate, "Extensions to the Modified Hydrodynamic Theory of Penetration," Preprint, to be published.

17. G. E. Hauver, "Penetration with Instrumented Rods," Int. J. Eng. Sci., 16, 871-877, 1978.

18. G. E. Hauver, "Experiments with Instrumented Long-Rod Penetrators," Fifth Int. Symp. Ballistics, Toulouse, France, 1980.

19. G. E. Hauver and A. Melani, "Strain-Gage Techniques for Studies of Projectiles During Penetration," ARBRL-MR-03082, Ballistic Research Laboratory, APG, MD, 1981 (AD A098660).

20. H. Kolsky, "Stress Waves in Solids," New York, Dover Publ., 1963.

21. P.-C. Chou, Letter Report to Ballistic Research Laboratory from Army Mechanics and Materials Research Center, 1980.

22. T. W. Wright, "Nonlinear Waves in Rods," Proc. IUTAM Symp. on Finite Elasticity, D. E. Carlson and R. T. Shield (eds.), The Hague, Boston, London, Nijhoff Publishers, 1980.

23. P. H. Netherwood, "Rate of Penetration Measurements," ARBRL-MR-02978, Ballistic Research Laboratory, APG, MD, 1979 (AD A080541).

24. P. H. Netherwood, Private Communication, 1979.

25. D. S. Pritchard, "Measurements of Dynamic Stress and Strain Components in Targets Struck by Penetrators," ARBRL-MR-03095, Ballistic Research Laboratory, APG, MD, 1981 (AD A100724).

26. D. S. Pritchard, "Piezoresistive Gauge Measurements in Deforming Environments During Penetration," Proc. First Symp. on Gauges and Piezoresistive Materials, Arcachon, France, 1981.

27. D. S. Pritchard and G. E. Hauver, Private Communication of Unpublished Data, 1982. The raw data were taken by Pritchard and reduced and analyzed by Hauver.

28. S. Hanagud and B. Ross, "Large Deformation, Deep Penetration Theory for a Compressible Strain-Hardening Target Material," AIAA Journal, 9, 905-911, 1971.

29. K. Frank, Private Communication on test results.

30. J. J. Misey, A. D. Gupta, and J. D. Wortman, "Comparison of Penetration Codes for Strain Measurements in Kinetic Energy Penetrators," ARBRL-TR-02231, Ballistic Research Laboratory, APG, MD, 1980 (AD A084391).

31. G. R. Abrahamson and J. N. Goodier, "Dynamic Flexural Buckling of Rods within an Axial Compression Wave," J. Appl. Mech., 33, 241-247, 1966.

32. J. A. Zukas, "Numerical Simulation of Impact Phenomena" (Chap 10), "Three-Dimensional Computer Codes for High Velocity Impact Simulation" (Chap 11), in Impact Dynamics, J. A. Zukas, T. Nicholas, H. F. Swift, L. B. Greszczuk, D. R. Curran, New York, Wiley-Interscience, 1982.

33. G. H. Jonas and J. A. Zukas, "Mechanics of Penetration: Analysis and Experiment," Int. J. Eng. Sci., 16, 879-903, 1978.

DISTRIBUTION LIST

No. of Copies	Organization
12	Administrator Defense Technical Info Center ATTN: DTIC-DDA Cameron Station Alexandria, VA 22314
2	Director Defense Advanced Research Projects Agency ATTN: Tech Info Dr. E. Van Reuth 1400 Wilson Boulevard Arlington, VA 22209
1	Deputy Assistant Secretary of the Army (R&D) Department of the Army Washington, DC 20310
1	HQDA (DAMA-ARP-P, Dr. Watson) Washington, DC 20310
1	HQDA (DAMA-MS) Washington, DC 20310
1	Commandant Command and General Staff College ATTN: Archives Fort Leavenworth, KS 66027
1	Commander US Army War College ATTN: Lib Carlisle Barracks, PA 17013
1	Commander US Army Materiel Development and Readiness Command ATTN: DRCDMD-ST 5001 Eisenhower Avenue Alexandria, VA 22333
1	Commander US Army Armament Research and Development Command ATTN: DRDAR-TDC (Dr. D. Gyorog) Dover, NJ 07801
7	Commander US Army Armament Research and Development Command ATTN: DRDAR-TSS DRDAR-LC, J. Frasier DRDAR-LCA, T. Davidson DRDAR-SC, J. D. Corrie J. Beetle E. Bloore Dover, NJ 07801
1	Director US Army Armament Research and Development Command Benet Weapons Laboratory ATTN: DRDAR-LCB-TL Watervliet, NY 12189
1	Commander US Army Armament Materiel Readiness Command ATTN: DRSAR-LEP-L Rock Island, IL 61299
6	Commander Benet Weapons Laboratory ATTN: Dr. M. A. Hussain Dr. Julian Wu Dr. John Underwood Mr. D. P. Kindall Dr. J. Throup Dr. E. Schneider Watervliet, NY 12189
1	Commander US Army Aviation Research and Development Command ATTN: DRDAV-E 4300 Goodfellow Boulevard St. Louis, MO 63120
1	Director US Army Air Mobility Research and Development Laboratory Ames Research Center Moffett Field, CA 94035

DISTRIBUTION LIST

No. of Copies	Organization
1	Commander US Army Communications Research and Development Command ATTN: DRSEL-ATDD Fort Monmouth, NJ 07703
1	Commander US Army Electronics Research and Development Command Technical Support Activity ATTN: DELSD-L Fort Monmouth, NJ 07703
1	Commander US Army Harry Diamond Laboratory ATTN: DELHD-TA-L 2800 Powder Mill Road Adelphi, MD 20783
1	Commander US Army Missile Command ATTN: DRSMI-R Redstone Arsenal, AL 35898
1	Commander US Army Missile Command ATTN: DRSMI-YDL Redstone Arsenal, AL 35898
2	Commander US Army Mobility Equipment Research & Development Command ATTN: DRDME-WC DRSME-RZT Fort Belvoir, VA 22060
1	Commander US Army Natick Research and Development Center ATTN: DRDNA-DT, Dr. D. Sieling Natick, MA 01762
1	Commander US Army Tank Automotive Command ATTN: DRSTA-TSL Warren, MI 48090
1	Director US Army TRADOC Systems Analysis Activity ATTN: ATAA-SL White Sands Missile Range NM 88002
1	Commander US Army Electronics Proving Ground ATTN: Tech Lib Fort Huachuca, AZ 85613
1	Director US Army BMD Advanced Technology Center ATTN: CRDABH-5, W. Loomis P. O. Box 1500, West Station Huntsville, AL 35804
3	Commander US Army Materials and Mechanics Research Center ATTN: DRXMR-T, J. Mescall DRXMR-T, R. Shea DRXMR-H, S. C. Chou Watertown, MA 02172
5	Commander US Army Research Office ATTN: Dr. R. Weigle Dr. E. Saibel Dr. G. Mayer Dr. F. Smiedeshoff Dr. J. Chandra P. O. Box 12211 Research Triangle Park, NC 27709
2	Commander US Army Research and Standardization Group (Europe) ATTN: Dr. B. Steverding Dr. F. Rothwarf Box 65 FPO NY 09510
2	Commandant US Army Infantry School ATTN: ATSH-CD-CSO-OR Fort Benning, GA 31905

DISTRIBUTION LIST

No. of Copies	Organization
2	Office of Naval Research Department of the Navy ATTN: Code 402 Washington, DC 20360
3	Commander US Naval Air Systems Command ATTN: AIR-604 Washington, DC 20360
1	Commander Naval Sea Systems Command Washington, DC 20362
3	Commander Naval Surface Weapons Center ATTN: Dr. W. H. Holt Dr. W. Mock DX-21- Lib Br Dahlgren, VA 22448
3	Commander Naval Surface Weapons Center ATTN: Dr. R. Crowe Code R32, Dr. S. Fishman Tech Lib Silver Spring, MD 20910
1	Commander and Director US Naval Electronics Laboratory ATTN: Lib San Diego, CA 92152
5	Commander US Naval Research Laboratory ATTN: C. Sanday R. J. Weimer Code 5270, F. MacDonald Code 2020, Tech Lib Code 7786, J. Baker Washington, DC 20375
7	Commander Naval Research Laboratory Engineering Materials Division ATTN: E. A. Lange G. R. Yoder C. A. Griffis R. J. Goode R. W. Judy, Jr. A. M. Sullivan T. W. Crooker Washington, DC 20375
4	Air Force Armament Laboratory ATTN: J. Foster John Collins Joe Smith Guy Spitale Eglin AFB, FL 32542
1	RADC (EMTLD, Lib) Griffiss AFB, NY 13440
1	AUL (3T-AUL-60-118) Maxwell AFB, AL 36112
2	Air Force Wright Aeronautical Laboratories Air Force Systems Command Materials Laboratory ATTN: Dr. Theodore Nicholas Dr. John P. Henderson Wright-Patterson AFB, OH 45433
1	Director Environmental Science Servi Administration US Department of Commerce Boulder, CO 80302
1	Director Lawrence Livermore Laboratory ATTN: Dr. M. L. Wilkins P. O. Box 808 Livermore, CA 94550

DISTRIBUTION LIST

No. of Copies	Organization
6	Sandia Laboratories ATTN: Dr. L. Davison Dr. P. Chen Dr. L. Bertholf Dr. W. Herrmann Dr. J. Nunziato Dr. S. Passman Albuquerque, NM 87115
1	Director Jet Propulsion Laboratory ATTN: Lib (TDS) 4800 Oak Grove Drive Pasadena, CA 91103
1	Director National Aeronautics and Space Administration Lyndon B. Johnson Space Center ATTN: Lib Houston, TX 77058
1	Aeronautical Research Associates of Princeton, Incorporated ATTN: Ray Gogolewski 1800 Old Meadow Rd., #114 McLean, VA 22102
1	Honeywell, Inc. Defense Systems Division ATTN: Dr. Gordon Johnson 600 Second Street, NE Hopkins, MN 55343
1	IBM Watson Research Center ATTN: R. A. Toupin Poughkeepsie, NY 12601
2	Orlando Technology, Inc. ATTN: Dr. Daniel Matuska Dr. John J. Osborn P. O. Box 855 Shalimar, FL 32579
7	SRI International ATTN: Dr. George R. Abrahamson Dr. Donald R. Curran Dr. Donald A. Shockey Dr. Lynn Seaman Mr. D. Erlich Dr. A. Florence Dr. R. Caligiuri 333 Ravenswood Avenue Menlo Park, CA 94025
1	System Planning Corporation ATTN: Mr. T. Hafer 1500 Wilson Boulevard Arlington, VA 22209
1	Terra Tek, Inc. ATTN: Dr. Arfon Jones 420 Wahara Way University Research Park Salt Lake City, UT 84108
3	California Institute of Technology Division of Engineering and Applied Science ATTN: Dr. J. Mikowitz Dr. E. Sternberg Dr. J. Knowles Pasadena, CA 91102
1	Denver Research Institute University of Denver ATTN: Dr. R. Recht P. O. Box 10127 Denver, CO 80210
3	Rensselaer Polytechnic Institute ATTN: Prof. E. H. Lee Prof. E. Krempl Prof. J. Flaherty Troy, NY 12181
1	Southwest Research Institute ATTN: Dr. Charles Anderson 8500 Culebra Road San Antonio, TX 78228

DISTRIBUTION LIST

No. of Copies	Organization
2	Southwest Research Institute Department of Mechanical Sciences ATTN: Dr. U. Lindholm Dr. W. Baker 8500 Culebra Road San Antonio, TX 78228
1	University of Dayton University of Dayton Rsch Inst ATTN: Dr. S. J. Bless Dayton, OH 45406
6	Brown University Division of Engineering ATTN: Prof. R. Clifton Prof. H. Kolsky Prof. L. B. Freund Prof. A. Needleman Prof. R. Asaro Prof. R. James Providence, RI 02912
3	Carnegie Mellon University Department of Mathematics ATTN: Dr. D. Owen Dr. M. E. Gurtin Dr. B. D. Coleman Pittsburgh, PA 15213
2	Catholic University of America School of Engineering and Architecture ATTN: Prof. A. Durelli Prof. J. McCoy Washington, DC 20017
2	Forrestal Research Center Aeronautical Engineering Lab. Princeton University ATTN: Dr. S. Lam Dr. A. Eringen Princeton, NJ 08540
1	Harvard University Division of Engineering and Applied Physics ATTN: Prof. J. R. Rice Cambridge, MA 02138
2	Iowa State University Engineering Research Laboratory ATTN: Dr. G. Nariboli Dr. A. Sedov Ames, IA 50010
2	Lehigh University Center for the Application of Mathematics ATTN: Dr. E. Varley Dr. R. Rivlin Bethlehem, PA 18015
1	New York University Department of Mathematics ATTN: Dr. J. Keller University Heights New York, NY 10053
1	North Carolina State University Department of Civil Engineering ATTN: Prof. Y. Horie Raleigh, NC 27607
1	Pennsylvania State University Engineering Mechanical Dept. ATTN: Prof. N. Davids University Park, PA 16502
2	Rice University ATTN: Dr. R. Bowen Dr. C. C. Wang P. O. Box 1892 Houston, TX 77001

DISTRIBUTION LIST

No. of Copies	Organization
1	Southern Methodist University Solid Mechanics Division ATTN: Prof. H. Watson Dallas, TX 75222
1	Temple University College of Engineering Technology ATTN: Dr. R. M. Haythornthwaite, Dean Philadelphia, PA 19122
4	The Johns Hopkins University ATTN: Prof. R. B. Pond, Sr. Prof. R. Green Prof. W. Sharpe Prof. J. Bell 34th and Charles Streets Baltimore, MD 21218
1	Tulane University Dept of Mechanical Engineering ATTN: Dr. S. Cowin New Orleans, LA 70112
3	University of California ATTN: Dr. M. Carroll Dr. W. Goldsmith Dr. P. Naghdi Berkeley, CA 94704
1	University of California Dept of Aerospace and Mechanical Engineering Science ATTN: Dr. Y. C. Fung P. O. Box 109 La Jolla, CA 92037
1	University of California Department of Mechanics ATTN: Dr. R. Stern 504 Hilgard Avenue Los Angeles, CA 90024
1	University of California at Santa Barbara Dept of Mechanical Engineering ATTN: Prof. T. P. Mitchel Santa Barbara, CA 93106
1	University of Delaware Dept of Mechanical Engineering ATTN: Prof. J. Vinson Newark, DE 19711
1	University of Delaware Dept of Mechanical and AErospace Engineering ATTN: Dr. Minoru Taya Newark, DE 19711
3	University of Florida Dept. of Engineering Science and Mechanics ATTN: Dr. C. A. Sciammarilla Dr. L. Malvern Dr. E. Walsh Gainesville, FL 32601
2	University of Houston Department of Mechanical Engineering ATTN: Dr. T. Wheeler Dr. R. Nachlinger Houston, TX 77004
1	University of Illinois Dept. of Theoretical and Applied Mechanics ATTN: Dr. D. Carlson Urbana, IL 61801
1	University of Illinois ATTN: Dean D. Drucker Urbana, IL 61801
1	University of Illinois at Chicago Circle College of Engineering Dept. of Materials Engineering ATTN: Dr. T. C. T. Ting P. O. Box 4348 Chicago, IL 60680
2	University of Kentucky Dept of Engineering Mechanics ATTN: Dr. M. Beatty Prof. O. Dillon, Jr. Lexington, KY 40506

DISTRIBUTION LIST

No. of Copies	Organization
1	University of Maryland Department of Mathematics ATTN: Prof. S. Antman College Park, MD 20742
1	University of Minnesota Dept of Aerospace Engineering and Mechanics ATTN: Prof. J. L. Erickson 107 Akerman Hall Minneapolis, MN 55455
1	University of Pennsylvania Towne School of Civil and Mechanical Engineering ATTN: Prof. Z. Hashin Philadelphia, PA 19105
4	University of Texas Department of Engineering Mechanics ATTN: Dr. M. Stern Dr. M. Bedford Prof. Ripperger Dr. J. T. Oden Austin, TX 78712
1	University of Washington Dept of Aeronautics and Astronautics ATTN: Dr. Ian M. Fyfe 206 Guggenheim Hall Seattle, WA 98105
2	Washington State University Department of Physics ATTN: Dr. R. Fowles Dr. G. Duvall Pullman, WA 99163
2	Yale University ATTN: Dr. B.-T. Chu Dr. E. Onat 400 Temple Street New Haven, CT 06520

No. of Copies	Organization
	Aberdeen Proving Ground
	Dir, USAMSAA ATTN: DRXSY-D DRXSY-MP, H. Cohen
	Cdr, USATECOM ATTN: DRSTE-TO-F
	Dir, USACSL, Bldg. E3516, EA ATTN: DRDAR-CLB-PA DRDAR-CLJ-L DRDAR-CLN

USER EVALUATION OF REPORT

Please take a few minutes to answer the questions below; tear out this sheet, fold as indicated, staple or tape closed, and place in the mail. Your comments will provide us with information for improving future reports.

1. BRL Report Number _____

2. Does this report satisfy a need? (Comment on purpose, related project, or other area of interest for which report will be used.)

_____

_____

_____

3. How, specifically, is the report being used? (Information source, design data or procedure, management procedure, source of ideas, etc.) _____

_____

_____

4. Has the information in this report led to any quantitative savings as far as man-hours/contract dollars saved, operating costs avoided, efficiencies achieved, etc.? If so, please elaborate.

_____

_____

5. General Comments (Indicate what you think should be changed to make this report and future reports of this type more responsive to your needs, more usable, improve readability, etc.) _____

_____

_____

_____

6. If you would like to be contacted by the personnel who prepared this report to raise specific questions or discuss the topic, please fill in the following information.

Name: _____

Telephone Number: _____

Organization Address: _____

_____

_____